

# ELECTRICALLY SMALL PLANAR ANTENNA FOR COMPACT ELECTROMAGNETIC (EM) WIRELESS ENERGY HARVESTING

Antwi Nimo<sup>\*</sup>, Dario Grgić and Leonhard M. Reindl

University of Freiburg – IMTEK, Department of Microsystems Engineering, Laboratory for Electrical Instrumentation, Freiburg, Germany

<sup>\*</sup>Presenting Author: antwi.nimo@imtek.de

**Abstract:** A high Q wireless energy harvester consisting of planar printed circuit board (PCB) antenna and a diode based radio frequency (RF) to direct current (DC) circuit is presented. The electrically small antenna, measures  $26 \text{ cm}^2$  with an efficiency of 8 % at 434 MHz and a measured gain of -8.6 dBi. The bandwidth of the antenna is 4 MHz with a quality factor (Q) of 108. The RF to DC circuit is optimized to a Q of 40 by matching the antenna and diode impedance with a PI network. By using a PI network, the harvester's (circuit) Q could be increased to enhance voltage transformation to the diode for better rectification and better efficiency at the load. At an antenna input power of  $0.316 \text{ } \mu\text{W}$ , the RF to DC operates at an efficiency of 16 % at  $1.6 \text{ k}\Omega$  load and more than 36 % at  $0.1 \text{ mW}$  for  $1.7 \text{ k}\Omega$  load.

**Keywords:** RF energy harvesting, electrically small antenna, RF to DC circuit, Diode impedance matching

## 1.0 INTRODUCTION

Micro energy harvesting has the potential to replace remote sensing elements requiring microwatt power levels for their operation. The use of other techniques (vibration/light/thermal) for micro energy harvesting is well presented [1]. EM power beaming has been proposed to transfer EM energy at far fields [2], but collimated EM energy in the form of laser beams are not common sources with which renewable energy harvesting can be based for wireless electromagnetic energy harvesting. The most common source of ambient EM energy is from telecommunications transmitting base stations in our environment. These energy sources are readily available in almost every remote environment. Electromagnetic wireless energy harvesting remains unexploited due to realistic difficulty in converting low EM power densities in ambient air to power remote wireless sensor nodes. The power density of the various renewable energy sources has been compared by [1]; EM energy density at far-field from a transmitting base station was reported to be in the order of  $0.3 \text{ } \mu\text{W}/\text{cm}^2$ . [3] has reported  $4 \text{ nW}/\text{cm}^2$  in ambient air at various frequencies. Wireless EM energy harvesters use antennas to receive the EM power and an RF to DC circuit and or power management circuit for powering wireless sensor nodes. To maximize the efficiency of EM harvesters, the coupling elements (transmit/receive antenna) must be optimal for maximum received power. Hence the receiving antenna is the first most important component in any wireless electromagnetic energy harvester. In microsystem applications, it is often the case that the physical size of a system be realized on the smallest possible area without performance trade-off. Since a 'good' antenna is directly related to its resonating wavelength, there is the need to find a good compromise between size constraint of microsystem applications and realistic performance for the antenna.

In this work, an ISM band 433 MHz - 434.7 MHz planar PCB antenna is presented for wireless electromagnetic energy harvesting applications. In addition to the antenna, an optimized diode based RF to DC circuit is presented to convert the captured EM power to usable DC, for wireless sensor nodes.

## 2.0 ANTENNA DESIGN AND SIMULATION

### 2.1 Antenna Design

The planar antenna is designed to find a good performance to size ratio at the ISM band 433-434.7 MHz. Richard Wallace [4] has presented PCB antennas at 433 MHz with helical wires which may not fit applications where planar structures are required. The presented antenna is realized on an FR4  $1 \text{ mm}$  substrate with the total antenna structure been realized on the PCB layers. The fabricated antenna is shown in Fig. 1. The length and width of the antenna is  $5.2 \text{ cm}$  and  $5 \text{ cm}$  respectively.

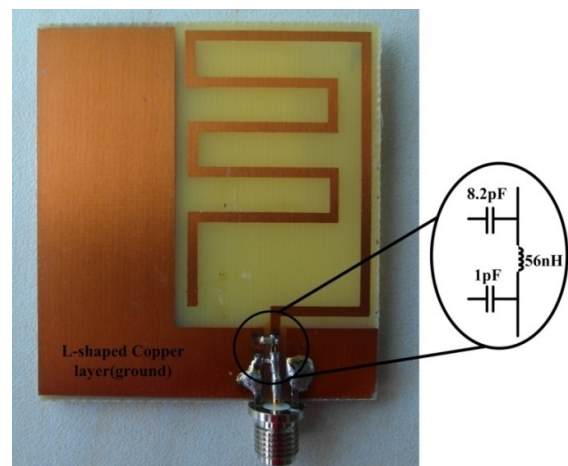


Fig. 1: FR4; thickness  $1 \text{ mm}$  434 MHz antenna ( $5.2 \text{ cm} \times 5 \text{ cm}$ ). A PI network consisting of  $1 \text{ pF}$ :  $56 \text{ nH}$ :  $8.2 \text{ pF}$  reactive elements are used to tune the antenna. Antenna backside has the same L-shaped copper layer.

A PI network (see Fig. 1) is used to tune the impedance and resonance frequency.

## 2.2 FEM simulation

The designed antenna was simulated in Ansoft's 3-D full-wave electromagnetic field software (HFSS) [5]. HFSS employs adaptive meshing through finite element method to calculate scattering parameters, resonant frequency and fields. A full 3-D model of the antenna was made. By using lumped LRC components, the PI network used to tune the antennas resonance frequency could be incorporated in the simulations for more accurate results. The next section of this work presents both measured and simulated results of the PCB 434 MHz planar antenna.

## 3.0 ANTENNA RESULTS

### 3.1 Reflection Coefficient measurements

Fig. 2 shows measured and simulated reflection coefficient ( $S_{11}$ ) of the antenna.

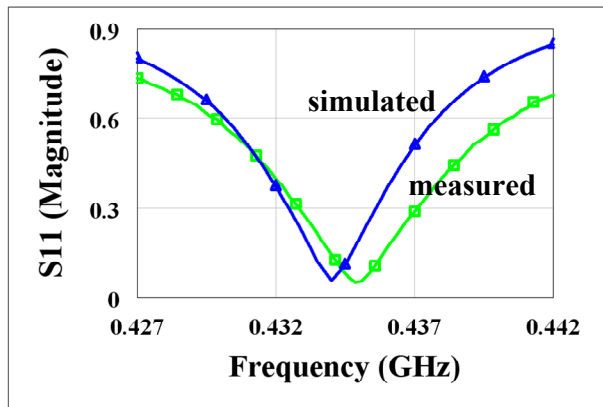


Fig. 2: Frequency sweep of the fabricated antenna vs.  $S_{11}$ ; reflection coefficient (magnitude), measured result (green), simulated result in HFSS (blue).

The minimum antenna reflection occurs at 434 MHz. The voltage standing wave ratio (VSWR) of 2:1 occurs between the band 431.7 MHz and 435.7 MHz. This corresponds to an antenna Q of about 108.

### 3.2 Impedance of Antenna

Since the impedance of the antenna must be matched to the impedance of the RF-DC circuit, the impedance of the antenna must be known or tuned to pure resistive to make impedance matching of the antenna to the RF to DC circuit easier. Fig. 3 shows measured and simulated impedance of the realized planar antenna. At 434 MHz, the impedance is  $55 (1.11 \times 50) + j0.85 (0.017 \times 50)$  which is resistive in any practical sense.

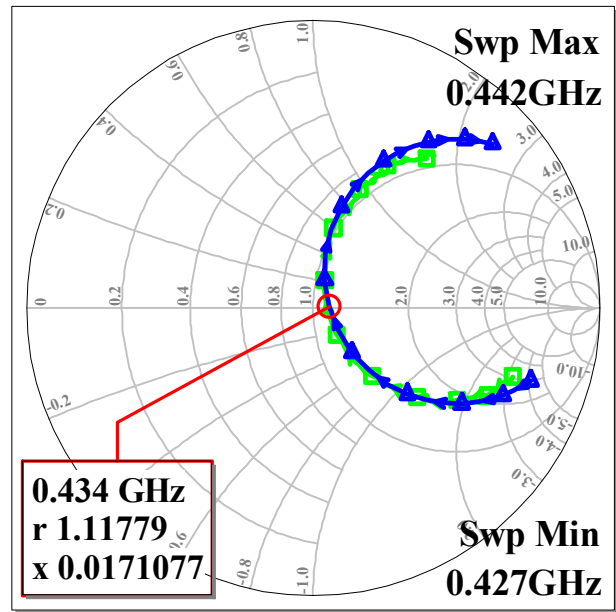


Fig. 3: Measured (green) and HFSS simulated (blue) impedance on a smith chart ( $50 \Omega$  normalized). At 434 MHz the measured impedance is  $55 + j 0.85$ .

### 3.3 Far field radiation, Gain and Efficiency

Fig. 4 shows simulated far field radiation pattern of the fabricated antenna (see Fig.1). The maximum simulated gain is  $-9.4$  dBi. The simulated efficiency is 8 %.

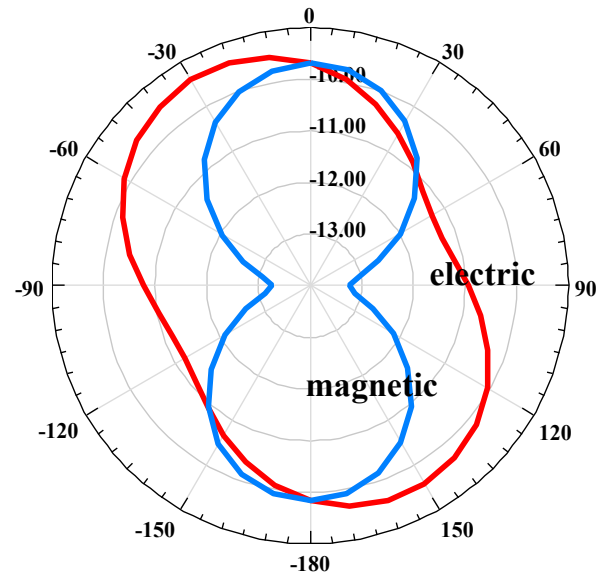


Fig. 4: Simulated electric field (red) and magnetic field (blue) at far field. Antenna maximum gain is  $-9.4$  dBi. Simulated radiation efficiency is 8 %.

Fig. 5 shows antenna received power versus distance from transmitter; the transmit/receive antennas were the same as in Fig. 1. The transmitting power was 1 mW at a frequency of 433 MHz. The experiment was done in an open space with the antennas raised high above the ground to prevent reflections. The antenna received power at far field (3 m at 433 MHz) is governed by the Friis law.

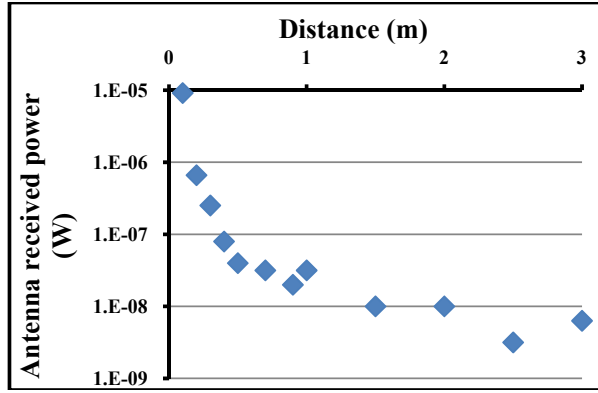


Fig. 5: Received antenna power over the distance for the same transmitting and receiving antenna (Fig.1). Transmitting power of 1 mW at 433 MHz

The Friis transmission equation gives the basis for calculating the antenna gain if the frequency, transmitted/receiving power and distance between the antennas are known; so long as the receiving antenna is at far-field relative to the transmitter ( $R \gg \lambda$  and  $R \gg$  transmitting antenna size). The Friis equation is given in equation 1.

$$\frac{P_r}{P_t} = G_t G_r \left( \frac{\lambda}{4\pi R} \right)^2 \quad (1)$$

where  $P_r$  is the received power,  $P_t$  is the transmitted power.  $G_t$  and  $G_r$  are the gain of transmitting and receiving antenna respectively,  $R$  is the distance between the transmitting and receiving antenna and  $\lambda$  is the wavelength of the transmitting signal.

Taking  $10 \log_{10}$  of both sides of equation 1 and equating the transmitting and receiving antenna gain's, the Friis equation can be written as in equation 2.

$$G = \frac{1}{2} \left[ 20 \log \left( \frac{4\pi R}{\lambda} \right) + 10 \log \left( \frac{P_r}{P_t} \right) \right] \quad (2)$$

where  $G$  is the gain of the transmitting or receiving antenna in dBi. At a distance of 3 m, the receiving antenna induces  $6.3 \times 10^{-9}$  W (-52 dBm) of power from the received signals transmitted at 433 MHz and 1 mW (Fig. 5). From these values,  $G$  turn out to be -8.6 dBi. This value compares well with the HFSS simulated values of -9.4 dBi.

#### 4.0 RF to DC CIRCUIT

The RF to DC wireless EM circuit consist of PI network in front of a zero biased Schottky diode; HSMS-285C [6]. Since diodes have non-linear impedance which varies as a function of input power level and connected load, a good matching network in-between antenna and diode is necessary to match the antennas impedance (50 - 55  $\Omega$ ) to the diodes impedance. A pi network is chosen to match the circuit impedance since the Q of the circuit can be defined.

By increasing the circuit Q, a voltage gain proportional to Q [7] is transformed (no power gain) which improves the rectification of the diode. For an ambient power density of  $0.3 \mu\text{W}/\text{cm}^2$  [1] available at an antenna of size  $26 \text{ cm}^2$  and an efficiency of 8-10 % (see Fig. 1 and 4),  $1 \mu\text{W}$  to  $0.1 \mu\text{W}$  range of power could be induced. Hence the RF to DC circuit is optimized for such low power levels. In order to prevent power losses and feedback of power into the diode, no resistor is used for tuning the RF to DC circuit and inductors are only used in series. A simulated (Quite Universal simulator) [8] impedance of the HSMS-285C diode at 50  $\Omega$ /  $0.1 \mu\text{W}$  input power was found to be  $110 - j685.44$ . This simulation is based on the HSMS-285C diode layout [9] and spice values of [6]. Based on this impedance and a desired circuit Q of 40, a PI network [10] as shown in Fig. 6 will match the antennas impedance ( $\sim 50\Omega$ ) to the HSMS-285C diode at that low power levels ( $0.1 \mu\text{W}$ ) for voltage gain to the diode and ultimately maximum efficiency of power to the load.

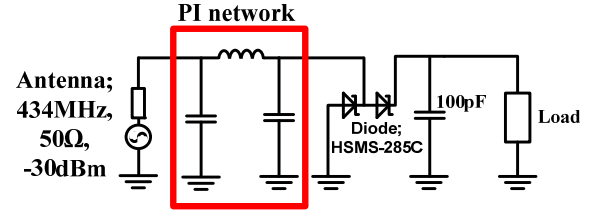


Fig. 6: RF to DC harvester schematic consisting of antenna, PI network (From left to right;  $30.5 \text{ pF}$ :  $44.2 \text{ nH}$ :  $2.8 \text{ pF}$ ) and HSMS-285C diode.

The values of the PI network as shown in Fig. 6 assume perfect matching of the characteristic impedance between various components in the circuit. These values have to be adjusted based on characteristic impedance (transmission lines on PCB) used to route the circuit and the availability of exact component on the market. For a strip-line transmission as shown in Fig 7 on an FR4 1.5 mm double coated PCB.

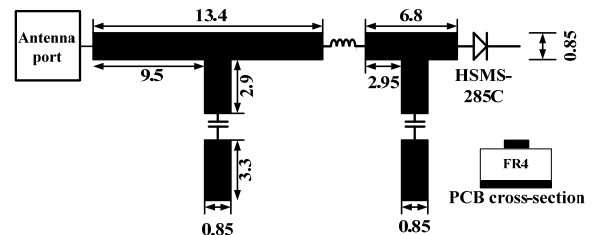


Fig. 7: Characteristic impedance of the RF to DC circuit optimized for  $1 \mu\text{W}$ . The black color represents the copper lines with dimensions in mm. The PI network consists of  $15 \text{ pF}$ :  $43 \text{ nH}$ :  $2 \text{ pF}$  from left to right. Bottom right shows the PCB cross-section.

The values of the components in the PI network change to  $15 \text{ pF}$ :  $43 \text{ nH}$ :  $2 \text{ pF}$  respectively.

## 4.1 RF to DC circuit results

### A. Circuit reflection coefficient

Measured reflection coefficient of the optimized circuit is shown in Fig. 8 (blue). The pink line in Fig. 8 is a circuit where the antenna's impedance ( $\sim 50 \Omega$ ) is fed directly to the diode.

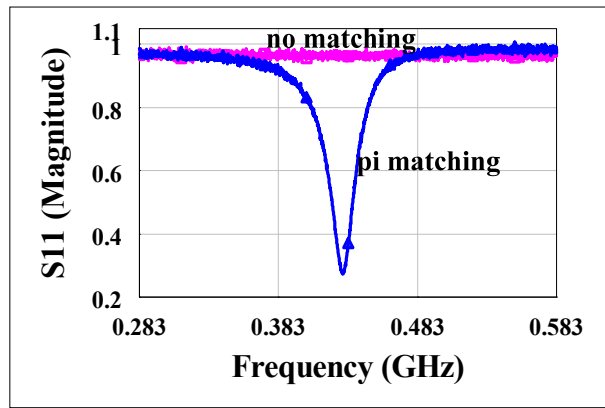


Fig. 8: Measured reflection coefficient of the RF-DC circuit at  $0.316 \mu\text{W}$  input power. PI network between antenna and diode (blue). Antenna impedance directly feeding the HSMS-285C diode (pink).

As can be seen from Fig. 8, there is minimal power reflection (reflection  $\sim 0.3$ ) with the optimized circuit (blue) around the ISM band 433 MHz while there is almost unity reflection of power by directly feeding the antenna impedance to the diode at  $0.316 \mu\text{W}$  between 200 MHz and 600 MHz. Measured circuit impedance changed from  $35 \Omega$  to  $50 \Omega$  from  $0.316 \mu\text{W}$  to  $0.1 \text{ mW}$  input power respectively. The discrepancy in the measured circuit impedance and the calculated PI values (see Fig 7) are due to the non linear nature of the diode (HSMS-285C) impedance and the unpreventable tolerance of RF components used to build the circuits.

### B. Efficiency of the RF to DC circuit

Fig. 9 shows the efficiency of the RF to DC (Fig. 7) circuit at various input power levels and loads from  $0.316 \mu\text{W}$  to  $0.1 \text{ mW}$ . A measured frequency sweep of the optimized RF to DC circuit indicated maximum sensitivity around 426 MHz for  $0.316 \mu\text{W}$  and around 427 MHz at  $0.1 \text{ mW}$  respectively. At  $0.316 \mu\text{W}$  (426 MHz) antenna input power, the circuit operates at an efficiency of 16 % at  $1.6 \text{ k}\Omega$ . This increases to more than 36 % at  $0.1 \text{ mW}$  for  $1.7 \text{ k}\Omega$ . 'Open' circuit voltage ( $\leq 0.5 \text{ M}\Omega$  load) is 50 mV for  $0.316 \mu\text{W}$  and 1.5 V for  $0.1 \text{ mW}$  input from antenna.

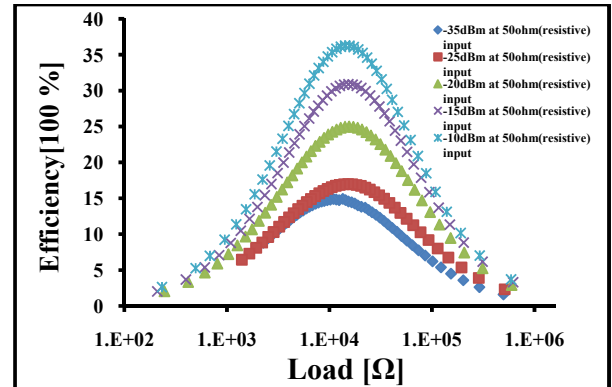


Fig. 9: Measured efficiency at different input power levels at 426 MHz.

## 5.0 CONCLUSION

A wireless EM micro energy harvester is presented, consisting of a planar ISM band 433 MHz antenna and an optimized RF to DC circuit. Antenna efficiency of 8 % ( $26 \text{ cm}^2$ ) and a gain of  $-8.6 \text{ dBi}$  are reported. An optimized RF to DC circuit can operate at an efficiency of 16 % at  $0.316 \mu\text{W}$  and more than 36 % at  $0.1 \text{ mW}$  for  $1.6 \text{ k}\Omega$  and  $1.7 \text{ k}\Omega$  respectively.

## ACKNOWLEDGEMENT

This work is part of the graduate program GRK 1322 Micro Energy Harvesting at IMTEK, funded by the German Research Foundation DFG. Special thanks to T. Ungan, T. Ostertag and F. Vollmer for technical assistance.

## REFERENCES

- [1] R.J.M. Vullers, R. van Schaijk, I. Doms, C. Van Hoof, R. Mertens, Micropower energy harvesting, Solid-State Electronics 53 (2009), pp. 684–693.
- [2] W.C. Brown, The history of power transmission by radio waves, IEEE Transactions on (1984), pp.1230–1242.
- [3] D. Bouchouicha et al, Ambient RF Energy Harvesting, International Conference on Renewable Energies and Power Quality (2010),pp. 1-4.
- [4] Richard Wallace, Texas Instruments Design Note DN031 (2010), pp. 20 and pp. 29.
- [5] Ansoft HFSS, www.ansoft.com/products/hf/hfss.
- [6] Avago Technologies, Data sheet HSMS-285x.
- [7] Franklin F. Kuo, Network Analysis and Synthesis (Second edition), Wiley International Edition (1962), pp. 225-238.
- [8] Quite universal circuit simulator, <http://qucs.sourceforge.net/index.html>.
- [9] Avago Technologies, Avago technologies Application Note 1124.
- [10] Chris Bowick, RF circuit design (Second edition), Newness press (2008), pp. 67-69.